45th AIAA/ASME/SAE/ASEE Joint Propulsion Conference & Exhibit
2 - 5 August 2009, Denver, Colorado

AIAA 2009-5065

Laser-Based Mass Flow Rate Sensor Onboard HIFiRE Flight 1

Shin-Juh Chen[1], Mark E. Paige[2], and Joel A. Silver[3]
Southwest Sciences, Inc., Santa Fe, NM 87505

Skip Williams[4] and Todd Barhorst[5]
Propulsion Directorate, Air Force Research Laboratory, WPAFB, OH 45433

The development of an optical mass capture sensor system for use onboard hypersonic flights under the HIFiRE program is discussed. The inlet flow velocity is determined directly from the Doppler shift of oxygen absorption lines centered about 760 nm with the use of wavelength modulation spectroscopy for high-sensitivity measurements. A compact, low weight and volume design are required for a flight-ready sensor system having minimum power consumption. The required tests for qualifying the instrument for flight are discussed. The sensor system completed successfully all qualification tests, and is on standby for launch 2010.

Nomenclature

α	=	absorption coefficient
f	=	modulation frequency
g	=	normalized line shape function or earth's gravity
I	=	transmitted light intensity
I_o	=	incident light intensity on the gas sample
l	=	optical path length
n	=	number density or harmonic
n	=	wavelength
S	=	absorption line strength
σ	=	absorption cross section
T	=	temperature

I. Introduction

The Hypersonic International Flight Research Experimentation (HIFiRE) program seeks to provide experimental requirements in the areas of physical and functional interfaces, spacecraft integration and test, and launch systems. The program also seeks to develop the first generation of compact diode laser systems capable of measuring oxygen concentration and velocity in the inlet or isolator section of a scramjet engine. The direct measurement of oxygen concentration via absorption spectroscopy and gas velocity via Doppler shift of laser light transmitting across the flowpath are needed. The deduced density-velocity product with a known area yields the mass flow rate. The precise knowledge of air mass capture is the most crucial parameter in trimming the engine for maximum thrust, fuel efficiency, and stability.

A hypersonic vehicle will be mounted within a sounding rocket payload and reach an apogee of about 300 km. The optical mass capture (OMC) system is expected to be functional during the ascent and descent phase of the flight path, below 30 km for maximum oxygen density. The peak Mach number during the flight is about 7.8. The total flight duration is around 560 sec. The rocket launches will occur in Woomera, Australia.

[1] Senior Research Scientist, 1570 Pacheco Street, Suite E-11, Senior Member.
[2] Principal Research Scientist, 1570 Pacheco Street, Suite E-11.
[3] Executive Vice President, 1570 Pacheco Street, Suite E-11.
[4] Deputy for Science, Aerospace Propulsion Division, AFRL/RZA, 1950 Fifth Street, Senior Member.
[5] Aerospace Engineer, AFRL/RZAS, 1950 Fifth Street, Member.

This paper discusses the development of an optical mass capture flight sensor that will be launched onboard a Terrier-Orion launch vehicle during HIFiRE Flight 1, scheduled for 2010. This sensor uses wavelength modulation spectroscopy (WMS) to obtain high-sensitivity measurements and is one of two OMC systems onboard. WMS shifts the detection band from DC to high frequencies where laser excess noise is unimportant, and absorbances near shot-noise limit can be achieved. Results of flight qualification tests, such as thermal cycling, vibration and shock, and vacuum, are provided.

The measurement technique and the associated hardware will be discussed at the system level. Specifically, the requirements necessitated a compact, low weight and volume design that could operate two lasers and four detectors and associated processing electronics on minimum power. The technical and flight qualification development of this one of a kind sensor system is discussed in detail.

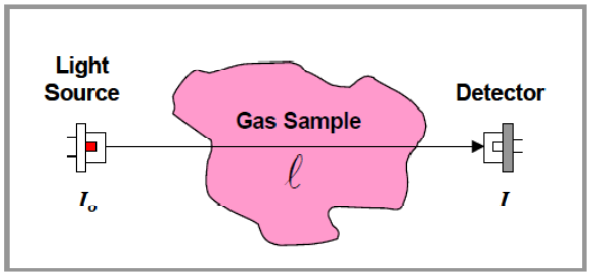

Figure 1. Schematic of laser-based absorption spectroscopy setup.

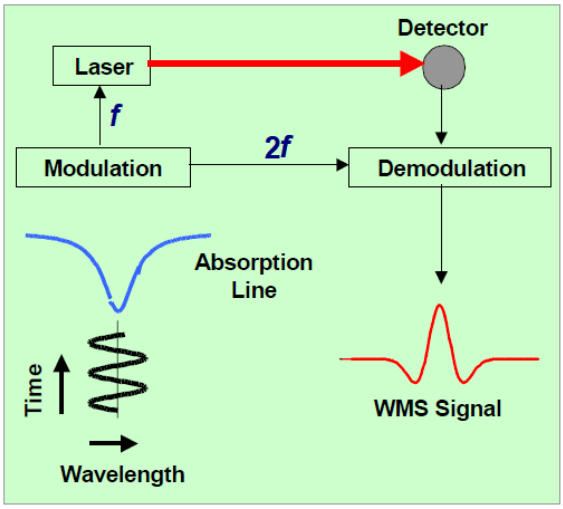

Figure 2. Schematic diagram for implementing wavelength modulation spectroscopy.

II. Wavelength Modulation Spectroscopy

A simple direct absorption spectrum using a diode laser is limited by low frequency noise, so that relative changes in the transmitted laser power of only 10^{-3} or greater can be detected. Techniques for achieving high sensitivity with diode lasers include wavelength modulation spectroscopy [1,2], frequency modulation spectroscopy [3], and "noise canceller" dual beam subtraction [4]. In all these techniques, the laser amplitude noise can be reduced to the theoretical shot noise limit. In practice, the noise in a spectral scan is dominated by coherent artifacts due to stray reflections in the optical path. These reflections interfere with the main laser beam ("etalon" effect) and produce sinusoidal ripples in the baseline.

The measurement of chemical species concentrations by diode laser absorption (see Figure 1) is based on straightforward implementation of Beer's law,

$$\frac{I}{I_o} = \exp(-\alpha)$$

$$\alpha = S(T)\, g(\nu)\, n\, l = \sigma(\nu)\, n\, l$$

where I_0 is the light intensity incident on the gas sample, I is the transmitted intensity and α the absorption coefficient. The absorption coefficient is comprised of the absorption line strength $S(T)$, the normalized line shape function $g(\upsilon)$, number density n in cm^{-3} and path length ℓ in cm. The line strength is a measure of how strongly light is absorbed and is a function of temperature but not pressure. The line shape function describes the wavelength dependence (υ) of the absorption and depends on both temperature and pressure. The absorption cross section term $\sigma(\upsilon)$ is the product of $S(T)$ and $g(\upsilon)$, and has units of cm^2. For conditions of varying temperatures, the line shape function is best described by a Voigt profile [5].

High-sensitivity has been achieved by using wavelength modulation spectroscopy to shift the detection band from DC (where laser amplitude noise can obscure weak absorbances) to high frequencies where laser excess ($1/f$) noise is unimportant. Fractional absorption sensitivities near the shot-noise limit (~10^{-7}) have been achieved in laboratory experiments [6]. Field measurements using WMS *routinely* maintain minimum detection absorbances of better than 10^{-5} (1 Hz bandwidth) for extended (many month) operation [7-9].

To implement WMS (see Figure 2), a small sinusoidal modulation at frequency f is superimposed on the diode laser injection current. This current modulation produces a modulation of the laser wavelength, since wavelength is tuned by changing the current. The amplitude of the current modulation is chosen so that the induced wavelength modulation is comparable to the width of the spectral feature under study. Absorption by the target gas converts the laser wavelength modulation to an amplitude modulation that induces ac components in the detector photo-current. Phase-sensitive electronics are then used to demodulate the detector photo-current at a selected harmonic, nf (typically, n = 2). Detection frequencies as low as 20 kHz are often sufficient to bypass laser excess noise. The signal from this detection method appears as approximately the second derivative of the absorption feature with respect to wavelength. Thus, 2f signals have a zero background. Fluctuations in the transmission due to slight misalignment or degradation of optical surfaces are accounted for by normalizing the 2f signal to the dc detector signal (I_o). Due to this linear intensity versus wavelength nature of these diode lasers, it turns out that the 1f signal is proportional to I_o. Thus, even for multiple lasers impinging on a single detector, each 2f signal can be properly normalized to its incident 1f dc level. A comparison of the detected signals between the direct method and wavelength modulation spectroscopy method is shown in Figure 3.

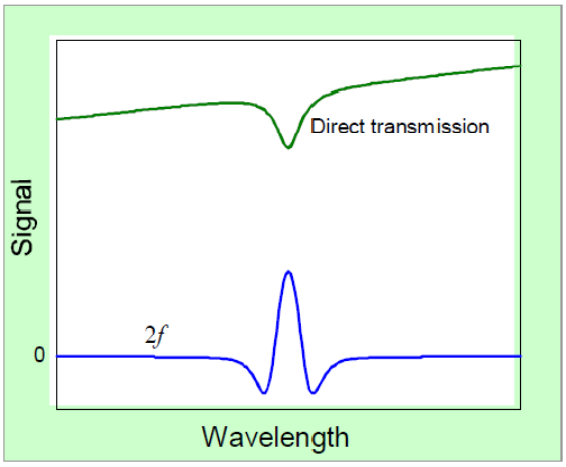

Figure 3. Comparison between direct and wavelength modulation spectroscopy.

III. Optical Mass Capture Flight Sensor

The OMC sensor measures 25.4 x 6.35 x 12.7 cm, and occupies a small volume of less than 2 L within the payload section of the launch vehicle. The sensor weighs less than 2 kg and consumes less than 2 W of power with a maximum current draw of less than 1 A. Onboard batteries provide 24 to 32 VDC. Two OMC sensors are shown in Figure 4.

Over the past twelve years, SWS has developed and refined a multi-purpose, stand-alone digital signal processor (DSP) board for wavelength modulation spectroscopy-based measurements of chemical species [6,10-12]. This board, upon application of 5V power, controls the laser scan, collects spectra, processes all data, and reports and/or stores the results in real-time. This component is the heart of the OMC system. The original application for the DSP board was for measurements of atmospheric moisture profiles using a weather balloon [13]. The system was designed for demanding specifications which included working over a wide dynamic concentration range (6 orders of magnitude), compactness, low power consumption, and the ability to work at temperatures down to –70°C and pressures as low as 0.05 atm. The DSP board has also been recently implemented into a handheld methane sensor and an airborne moisture sensor.

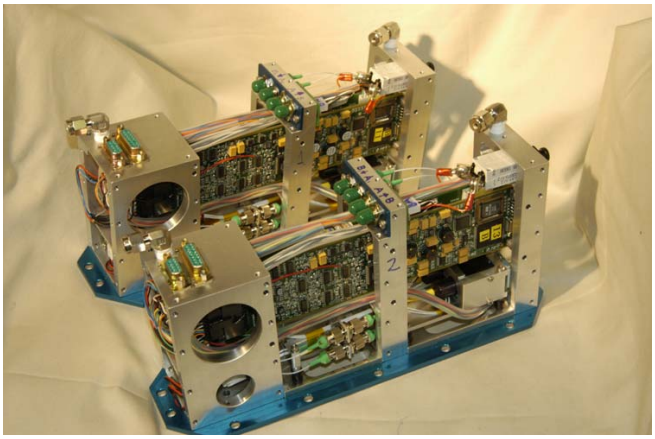

Figure 4. Two flight-ready OMC sensors developed by Southwest Sciences.

The DSP board has a 100 MIP, fixed-point 16-bit DSP processor. The onboard A/D converter is a 400 kHz, 8 channel, 12-bit chip and the D/A converter is a 333 kHz, 4 channel, 12-bit chip. The system performs laser current and temperature control for a distributed feedback (DFB) laser or vertical cavity surface emitting laser (VCSEL), has two photodiode channels with lock-in amplifiers, fits spectral data, and provides 3.3 V logic level serial output up to 19.6 kbaud. Laser temperature is controlled within 0.01°C. In general, fine temperature control is performed using feedback from the spectral signal (keeping the peak centered in the wavelength scan). An 8-bit divider of the 100 MHz DSP clock is used to set the modulation frequency. The laser wavelength is generally stepped at a 100 -

150 kHz rate. Automatic gain adjustment of the signal levels is provided with a switchable 4-level pre-amplifier, and two post lock-in digitally adjustable amplifiers.

The sensor utilizes two fiberized vertical cavity surface emitting lasers (VCSEL) to provide two laser beams for velocity measurements within the duct assembly. The lower section of the sensor package contains two independent laser systems sharing a reference cell for line-locking purposes. Each laser beam is split into two beams. One is for the measurement path, and the other beam is for the reference path. The reference cell contains two silicon photodiode detectors for the reference cell signals. Two digital signal processing boards (DSP), located in the upper section of the sensor, are used to control the lasers, collect and process laser signals returning from the duct assembly and reference cell. Fiber optic cables bring the laser beams to near the walls of the duct assembly. Another two fiber optic cables, connected to fiberized silicon photodiodes, collect the transmitted laser beams for analysis.

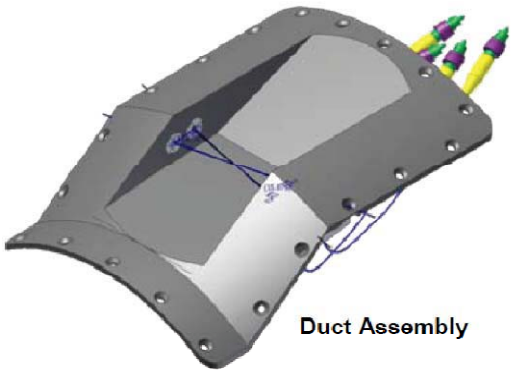

Figure 5. Duct assembly showing two laser paths across the duct with a pitch-and-catch fiber optics system.

The duct is shown in Figure 5 where two laser beam paths crossed each other. This arrangement allows the gas velocity to be measured using both beams without the need to correct for pressure shift of the absorption line. The measured Doppler shift is then directly proportional to the gas velocity. Special collection optics with rugged sheathing for the optical fibers, developed by AFRL and Zolo Technologies, is used to send and receive the laser beams from the duct assembly. The collected spectra are sent to the flight computer via RS-485 lines and high-speed A/D channels. Data are downloaded to ground station via telemetry. Two purge ports are located on top of the sensor for nitrogen gas flows to prevent water condensation during wet days as the instrument is shipped to launch site or awaiting launch. A companion paper [14] discusses the development of flight vehicle, duct assembly, and optical assembly within the duct.

IV. Sensor Qualification Tests

Component qualification tests were conducted to demonstrate the flight-worthiness of the OMC sensor. These tests included atmospheric pressure, thermal cycling, vibration and shock, vacuum, and corona check. Specifications for each of the tests are outlined in the NSROC Environmental Testing Policy Manual.

A. Atmospheric Pressure Tests

Prior to launch, the onboard pressure transducers are calibrated by pressurizing the payload section up to 300 kPa (3 atm absolute). The system must be shown to tolerate this pressure condition within the payload section of the rocket. The OMC unit was tested in two separate parts since the pressure chamber could not accommodate the complete OMC sensor. The frame and the upper section of the unit were first tested, followed by the lower section of the unit. The lower section includes the reference cell, fiber optic cables and splitters, and one laser. The components were inserted into a chamber, and air pressure was raised to 30 psig and kept for 25 minutes. After the test, the reference cell windows remain intact, and the peak 2*f* signal of the reference cell is unchanged.

B. Reference Cell Leak Tests

A reference cell containing a mixture of 75% O_2 and 25% N_2 resides in the lower section of the sensor unit. This cell serves to lock the laser wavelength when regions of low oxygen concentrations are encountered during flight. The ends of the reference cell have o-ring sealed optical windows. Two fiber collimators are attached in one end, and two silicon photodiode detectors in the other end.

During the test the internal pressure of the reference cell dropped from 613 to 605 torr in a vacuum chamber pressure of about 0.045 torr over a time period of 24 hours. The drop in pressure is primarily due to the plumbing components used during the leak test to monitor the vacuum chamber and reference cell internal pressures. The reference cell was filled over a year ago, and the measured signal strengths are still within the reasonable range.

C. Vibration and Shock Tests

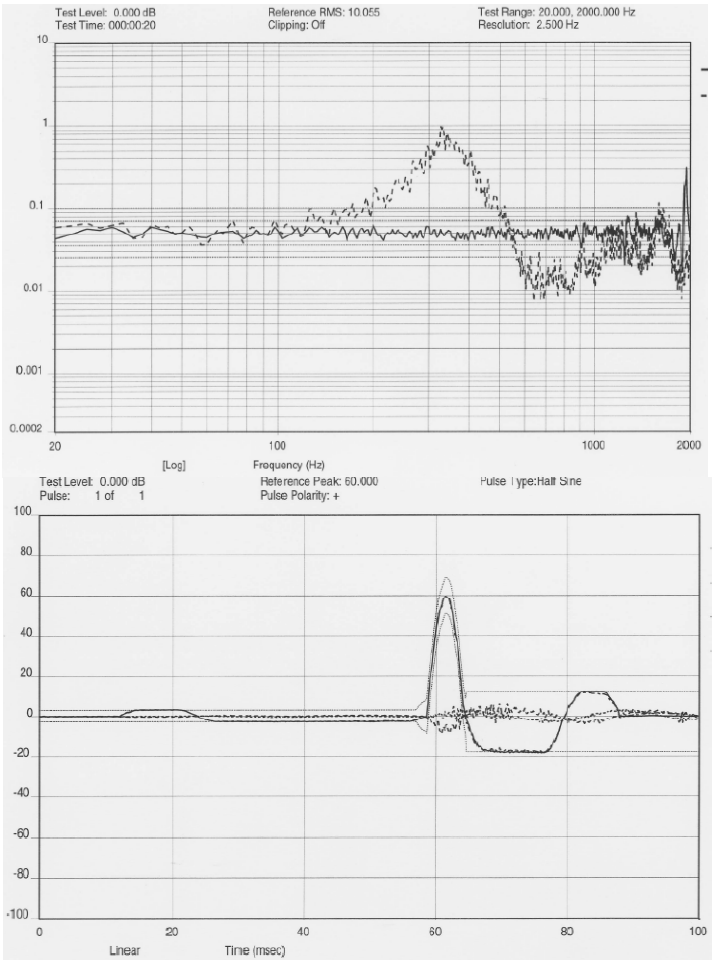

Figure 6. Mechanical responses of OMC sensor due to random vibration along the Z-axis (top), and positive shock along the Z-axis (bottom).

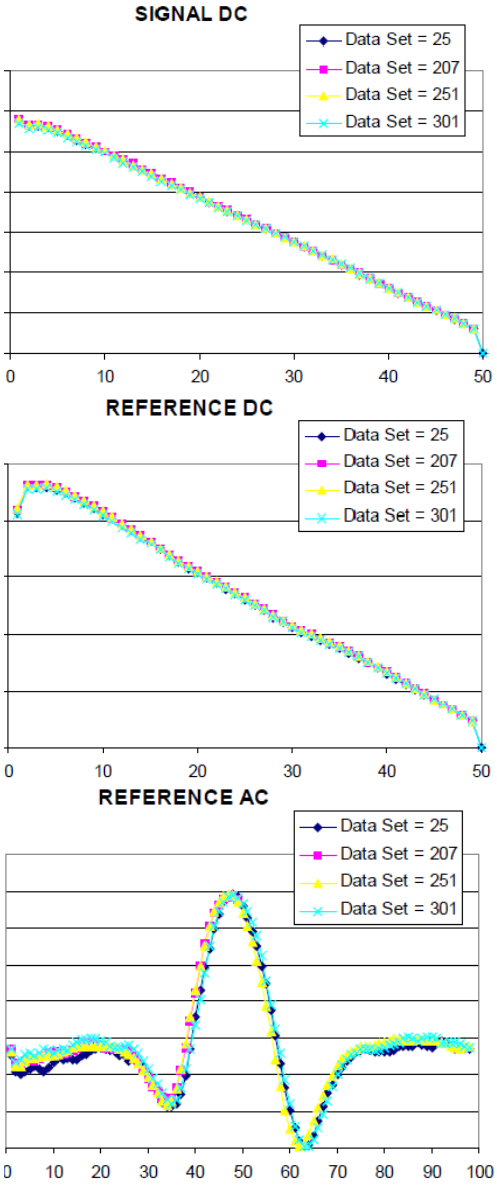

Figure 7. Responses of laser to random vibration along the Z-axis. The reference DC (top) and AC (middle), as well as the signal DC (bottom) are shown.

Vibration and shock tests were conducted in all three axes. Both random and sine wave vibration were completed. Along the X and Y-axis (lateral), the sine sweep rate is 4 oct/min. For frequency range between 10-35 Hz, +/- 0.075 m/sec (3 in/sec) velocity was used. For 35-105 Hz, +/- 7g acceleration was used. For 105-2000 Hz, +/- 5g acceleration was used. Along the Z-axis (thrust), the sine sweep rate is 4 oct/min. For 10-144 Hz, +/- 0.075 m/sec (3 in/sec) velocity was used. For 144-2000 Hz, +/-7g acceleration was used.

Random vibration along the X and Y-axis was conducted for a period of 20 sec per axis, at 7.6 grms, with 0.029 g^2/Hz acceleration for frequency between 20 to 2000 Hz. Along the Z-axis, test was conducted for 20 sec with 10.0 grms, with 0.051 g^2/Hz acceleration for frequency between 20 to 2000 Hz.

In all three axes, shock tests were conducted at a minimum of two tests per axis. Shock input was +/-60 g for a duration of 6 msec using a half-sine pulse type.

A typical result obtained during a random vibration cycle, at 10 g's RMS and positive 60 g shock, along the thrust-axis is shown in Figure 6. For the random vibration test, the g-sensor was placed on one chip of the DSP board. The solid line is the control, and the dashed line is the response of the chip. For the shock test, the solid line is the control, dotted line is the X-axis response, dashed line is the Y-axis response, and the dashed-dotted line is the Z-axis response. The associated laser responses to the random vibration and shock are shown in Figure 7 and 8. An accelerometer was attached to one of the DSP boards to monitor its response during the cycle. There were no

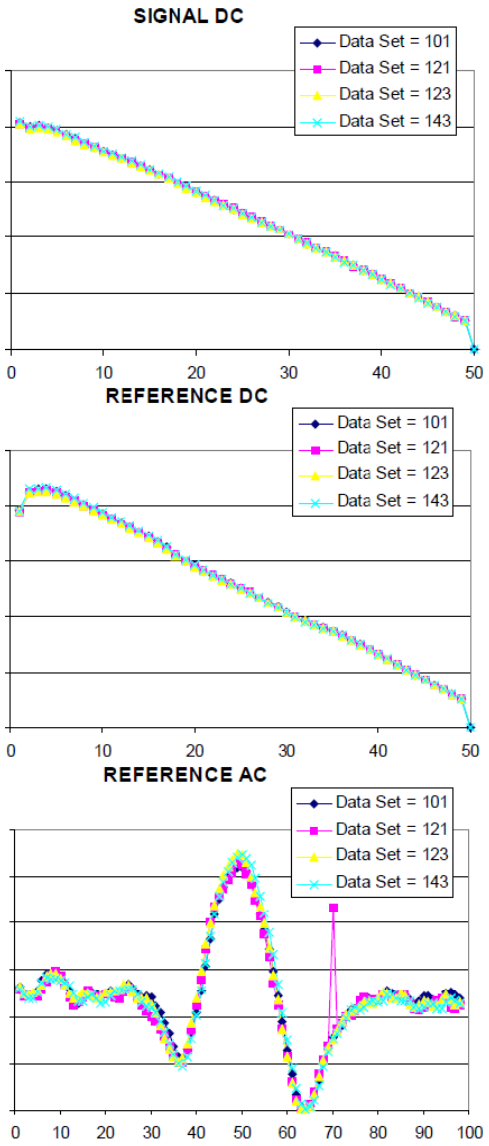

Figure 8. Responses of laser to positive shock along the Z-axis. The reference DC (top) and AC (middle), as well as the signal DC (bottom) are shown.

Figure 10 shows the effect of temperature variation on four different lasers. These four lasers do not respond to the temperature changes the same way. Lasers having steady output power over the tested temperature range are selected and incorporated into the OMC sensor units.

In each case of the thermal cycling tests, the high temperature exposure precedes the low temperature exposure. During the operational test, the component is turned on throughout the temperature transitions, which takes place at 1 °C/min. When the component reaches steady state, which is

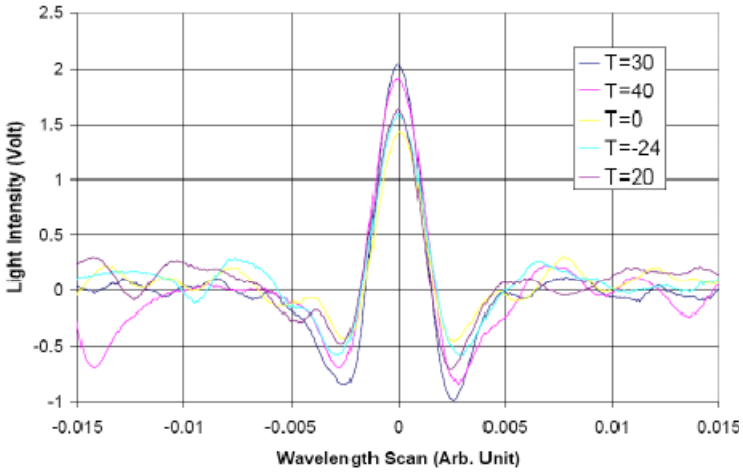

Figure 9. Effect of ambient temperature on the 2*f* line shape.

significant resonances observed, and the sensor did not experience any mechanical failures during all the vibration tests, including sine and random, in all three independent axes. Other accelerometers were placed in other locations within the sensor to monitor their responses. The sensor package met all requirements for vibrations and shock.

D. Thermal Cycling Tests

The effect of ambient temperature, ranging from +40 to –24°C, on the peak laser light intensity is shown on Figure 9 for one laser. The fiberized lasers contain an epoxy to set the optical components within the laser module. Each fiberized laser was thermally tested to assess the effect on temperature on the output power. The collected WMS spectra were manually centered at 0 so that all curves fall on top of each other for ease of comparison. The important thing to be noted here is that there are no thermally-induced etalons present.

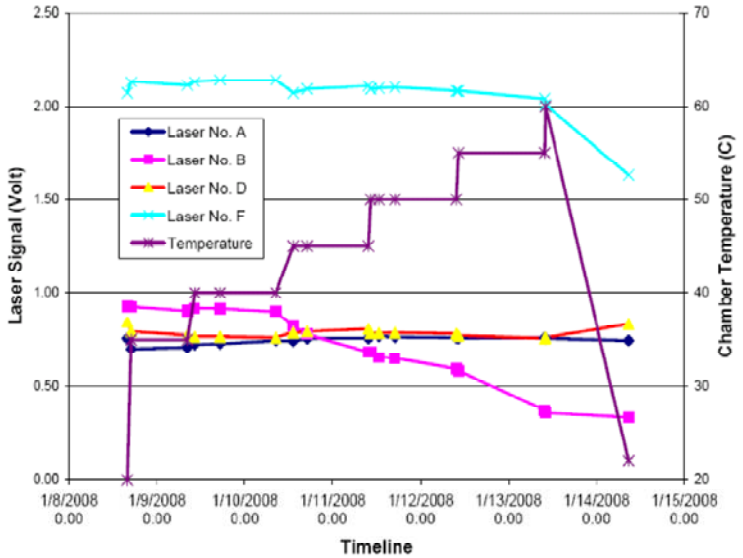

Figure 10. Effect of temperature on the power output of four lasers.

defined as less than 3 °C/hr temperature change, the OMC sensor is turned off and turned back on at least once. The component is operated in between cycles and at the end of cycling for at least 30 minutes. The high and low temperatures were +61°C and –24°C, respectively. A total of six thermal cycles is required.

The laser is not required to operate below 0 °C. The system is turned off as the temperature falls below 0 °C to reach –24°C. As the temperature is cycled back to 0°C, the laser system is turned on. The sensor package met all requirements for thermal cycling.

E. Corona Check Tests

The OMC sensor unit was inserted into a pressure vessel. A vacuum pump drew the pressure down to about 0.1 torr. The unit was turned on and left alone for three hours (exceeding the 1 hr requirement). The voltage and current draw remained the same at 25 VDC and 50 mA. Note that the laser was not turned on. Only the DSP boards were turned on. All relevant serial outputs were reading normal. Based on the results, the unit passed the corona check.

V. Conclusion

This project's ultimate goal is to develop first generation compact diode laser systems capable of measuring the mass flow rate in the inlet or isolator of a hypersonic vehicle mounted within a sounding rocket payload over an altitude range of 60,000-90,000 ft. A compact, low-power, low weight and volume, high-sensitivity optical mass capture sensor was developed and completed all necessary qualification tests. These tests included atmospheric pressure, vibration and shock, thermal cycling, and corona check. The sensor occupied a volume of less than 2 L, weighed less than 2 kg, and consumed less than 2 W of power. The OMC sensor will be launched onboard a sounding rocket in 2010 in Woomera, Australia.

Acknowledgments

This project is supported by the U.S. Air Force Research Laboratory (AFRL), Wright-Patterson Air Force Base, Ohio, under a subcontract from Universal Technology Corporation (UTC).

References

[1]Silver, J. A., *J. Appl. Opt.* **31**, 707-717, 1992.

[2]Bomse, D. S., Stanton, A. C., and Silver, J. A., *Appl. Opt.* **31**, 718-731, 1992.

[3]Carlisle, C.B., D.E. Cooper, *Appl. Opt.* **28**, 2567–2576, 1989.

[4]Sonnenfroh, D.M., Sewell, S.D., Allen, M.G., in Application of Tunable Diode and Other Infrared Sources for Atmospheric Studies and Industrial Process Monitoring, *SPIE Proceedings* **2834,** 57–66, 1996.

[5]Hui, A. K. Amstrong, B. H., and Wray, A. A., *J. Quant. Spectrosc. Radiat. Transfer* **19**, 509-516, 1978.

[6]Bomse, D. S., Stanton, A. C., and Silver, J. A., *Appl. Opt.* **31**, 718-731, 1992.

[7]Stanton, A. C., Silver, J. A., Bomse, D. S., Oh, D. B., Hovde, D. C., Paige, M. E., and Kane, D. J., in *Application of Tunable Diode and Other Infrared Sources for Atmospheric Studies and Industrial Process Monitoring*, A. Fried, ed., *Proc. SPIE* **2834**, 41, 1996.

[8]Silver, J. A. and Hovde, D. C., Rev. Sci. Instrum. **65**, 1691-1694, 1994.

[9]Hovde, D. C., Meyers, T. P., Stanton, A. C. and Matt, D. R., *J. Atmos. Chem.* **20**, 141, 1995.

[10]Silver, J. A. and Stanton, A. C., "Two-Tone Optical Heterodyne Spectroscopy Using Buried Double Heterostructure Lead-Salt Diode Lasers," *Appl. Opt.* **27**, 4438, 1988.

[11]Silver, J.A., "Frequency Modulation Spectroscopy for Trace Species Detection: Theory and Comparison Among Experimental Methods," *J. Appl. Opt.* **31**, 707-717, 1992.

[12]Silver J.A., Kane, D.J., and Greenberg, P.S., "Quantitative Species Measurements in Microgravity Flames with Near-IR Diode Lasers," *Appl. Opt.* **34**, 2787, 1995.

[13]Paige, M.E., "Compact and Low-Power Diode Laser Hygrometer for Weather Balloons," *J. Atmos. Oceanic Technol.* 22, 1219 – 1224, 2005.

[14]Barhorst, T., Williams, S., Chen, S.-J., Paige, M.E., Silver, J.A., Sappey, A., McCormick, P., Masterson, P., Zhao, Q., Sutherland, L., Smith, I., VanHoudt, P., Hannam, J., and Owenby, D., "Development of an In Flight Non-Intrusive Mass Capture System," AIAA Paper No. 2009-5067, AIAA Joint Propulsion Conference, AIAA, Washington, D.C., 2009.